Current Research in Food Science 8 (2024) 100726

Contents lists available at ScienceDirect

Current Research in Food Science

journal homepage: www.sciencedirect.com/journal/current-research-in-food-science

Trace level detection of melamine and cyanuric acid extracted from pet liquid food (milk) using a SERS Au nanogap substrate

Rahul Joshi[a,1], Samir Adhikari[b,1], Minjun Kim[b], Yudong Jang[c], Hyun Jung Min[d], Donghan Lee[b,c,**], Byoung-Kwan Cho[a,e,*]

[a] Department of Biosystems Machinery Engineering, Chungnam National University, 99 Daehak-to, Yuseong-gu, Daejeon, 34134, South Korea
[b] Department of Physics, Chungnam National University, Daejeon, 34134, South Korea
[c] Institute of Quantum Systems, Chungnam National University, Daejeon, 34134, South Korea
[d] Department of Mechanical Engineering, Purdue University, IN, 47907, USA
[e] Department of Smart Agriculture Systems, College of Agricultural and Life Science, Chungnam National University, 99 Daehak-to, Yuseong-gu, Daejeon, 34134, South Korea

ARTICLE INFO

Handling Editor: Professor Aiqian Ye

Keywords:
Surface-enhanced Raman spectroscopy
Au nanogap
Melamine
Cyanuric acid
PLSR
Variable importance in projection (VIP)

ABSTRACT

This study reported an application of Au nanogap substrates for surface-enhanced Raman scattering (SERS) measurements to quantitatively analyze melamine and its derivative products at trace levels in pet liquid food (milk) combined with a waveband selection approach, namely variable importance in projection (VIP). Six different concentrations of melamine, cyanuric acid, and melamine combined with cyanuric acid were created, and SERS spectra were acquired from 550 to 1620cm^{-1}. Detection was possible up to 200 pM for melamine-contaminated samples, and 400 pM concentration detection for other two groups. The VIP-PLSR models obtained correlation coefficient (R^2) values of 0.997, 0.985, and 0.981, with root mean square error of prediction (RMSEP) values of 18.492 pM, 19.777 pM, and 15.124 pM for prediction datasets. Additionally, partial least square discriminant analysis (PLS-DA) was used to classify both pure and different concentrations of spiked samples. The results showed that the maximum classification accuracy for melamine was 100%, for cyanuric acid it was 96%, and for melamine coupled with cyanuric acid it was 95%. The results obtained clearly demonstrated that the Au nanogap substrate offers low-concentration, rapid, and efficient detection of hazardous additive chemicals in pet consuming liquid food.

1. Introduction

The purposeful addition of harmful ingredients or additions to food products in order to make profit is recognized as a source of concern in the modern world. Food security protocols include issues that need to be addressed, as demonstrated through various past incidents. In 2007 the US Food and Drug Administration (FDA) found melamine in pet food imported from China, which was one well-known example of food falsification. Following the ingestion of melamine-contaminated food, this revelation resulted in the sickness and death of several dogs (Abbas et al., 2013). In 2008, melamine was fraudulently added to infant milk powders that were also provided by China, resulting in 50,000 hospital admissions and the deaths of six children (De Lourdes Mendes Finete et al., 2013; Miao et al., 2009). Due to their numerous beneficial qualities, both melamine and cyanuric acid are commonly used as industrial chemicals. Additionally, both compounds are nitrogen-efficient molecules, as shown in Fig. 1a and b, which has resulted in their inclusion in human and pet food products to increase the nitrogen content (Rovina and Siddiquee, 2015; Patel and Jones, 2007). Melamine and cyanuric acid have relatively little toxicity when consumed independently, but when combined, they have a strong affinity for one another, resulting in the formation of the barely soluble melamine-cyanurate complex (Ranganathan et al., 1999; Bielejewska et al., 2001) as shown in Fig. 1c. Melamine and cyanurate together have been linked to severe chronic

* Corresponding author. Department of Biosystems Machinery Engineering, Chungnam National University, 99 Daehak-to, Yuseong-gu, Daejeon, 34134, South Korea.
** Corresponding author. Department of Physics, Chungnam National University, Daejeon, 34134, South Korea.
E-mail addresses: dlee@cnu.ac.kr (D. Lee), chobk@cnu.ac.kr (B.-K. Cho).
[1] Equal contribution.

https://doi.org/10.1016/j.crfs.2024.100726
Received 28 November 2023; Received in revised form 26 February 2024; Accepted 26 March 2024
Available online 30 March 2024

kidney inflammation, renal failure caused by blockage, and kidney and bladder stones, according to earlier research (Stine et al., 2014; Kuo et al., 2013; Dorne et al., 2013).

Conventional approaches for cyanuric acid and melamine detection mostly entail wet chemistry methods such as gas chromatography-tandem mass spectrometry (Miao et al., 2009) and high-performance liquid chromatography (HPLC) (Filazi et al., 2012). Moreover, utilizing capillary electrophoresis-diode array detection technique (CE-DAD) with a limit of quantification (LOQ) of 0.20 ug/ml, several researchers have investigated melamine in milk and milk powder (Chen and Yan, 2009), and in milk samples using matrix-assisted laser desorption/ionization combined with time-of-flight mass spectrometry (MALDI--TOFMS) with a 0.10 mg/kg detection limit (Su et al., 2013). All of these aforementioned techniques offer a lower limit of detection (means the instrument could detect analytes presents in lower concentrations), higher sensitivity, and higher limit of quantification properties. However, their time-consuming, destructive, and complex sample preparation limit their applicability in the real time-monitoring of products.

Due of the weak Raman effect, traditional Raman spectroscopy is not as applicable for detecting low concentration levels. In 1974, a team of researchers from the United Kingdom introduced a novel phenomenon called surface-enhanced Raman spectroscopy, which aimed to address the limitation of Raman spectroscopy for the detection of pesticides or harmful chemicals present in low concentration ranges. The researchers observed an increase in Raman signal intensity for pyridine molecules coated on an electrochemically roughened Ag electrode surface (Fleischmann et al., 1974). Modern nanotechnology and the creation of very sensitive substrates have led to the employment of SERS in medicine, agricultural products, and biological science (Yilmaz and Culha, 2022; Fan et al., 2015), (P. Wang et al., 2016) as evidenced by a number of recent studies. The application of machine learning techniques becomes crucial in order to extract the critical information included in the SERS spectrum data. Even though SERS spectroscopy is a popular technique for assessing the quality of food and agricultural goods, chemometrics is required to uncover relevant hidden information in the spectrum data. Therefore, the main objectives of this study might be explained by the following two current statements:

1) To evaluate the feasibility of using the SERS Au nanogap substrate for the picomolar range measurement of melamine, cyanuric acid, and their combination in pet liquid meals (milk).
2) Variable importance in the projection (VIP), in conjunction with the partial least squares regression approach and hybrid linear analysis, was used as a variable selection methodology in order to identify significant variables and increase model prediction accuracy by reducing computation time.

2. Materials and methods

2.1. Chemicals

For the purpose of this research, 99% pure cyanuric acid and melamine were purchased from Sigma-Aldrich in St. Louis, Missouri, USA. Additionally, pet food was brought from a nearby veterinary clinic in the form of pet liquid food (milk).

2.2. Preparation of standard solution, mango juice, and milk samples

For this investigation, melamine and cyanuric acid powder were first mixed in deionized water (DI). The limit of detection for this SERS Au nanogap substrate was tested by varying the amounts of melamine, cyanuric acid, and melamine coupled with cyanuric acid. The first step involved making a 1 μM stock solution with DI water as the solvent and stirring it for almost 3 h. Melamine was spiked into the liquid diet, and each milk sample at various levels (1200 pM, 1000 pM, 800 pM, 600 pM, 400 pM, and 200 pM) was diluted from the 1 μM stock solution. Similarly, 1 μM Cyanuric acid stock solution was made with DI water as a solvent and stirred for almost 3 h. The liquid diet and each milk were mixed with cyanuric acid at different concentrations: 1200 pM, 1000 pM, 800 pM, 600 pM, 400 pM, and 200 pM. Using a Sorvall Biofuge Primo Centrifuge from Thermo Electron Corporation, all of the liquids are centrifuged for 30 min at 7000 rpm. Before SERS measurements, a 5 cm by 5 cm au leaky NG sample was coated with supernatants and dried with nitrogen gas. On the other hand, pure veterinary feed (milk) that is free of cyanuric acid, melamine, and melamine mixed was also prepared during this experiment.

2.3. Nanogap SERS substrates

We employed very sensitive and uniform wafer-scale gold nanogap SERS substrates, made using the techniques outlined in (Adhikari et al., 2022). The fabrication process was completed in three simple steps: Au deposition, rapid thermal annealing, and wet chemical etching. Fig. 2a shows a schematic representation of an Au nanogap substrates. Au nanospheres were perched above SiO_2 nanopillars in the substrate, as shown in Fig. 2b, with nanogaps separating the nanospheres from the bottom Au film. The nanogap distance may be accurately regulated by modifying the etch depth and the thickness of the Au film. This nanogap SERS substrate demonstrated exceptional uniformity over a 6-inch

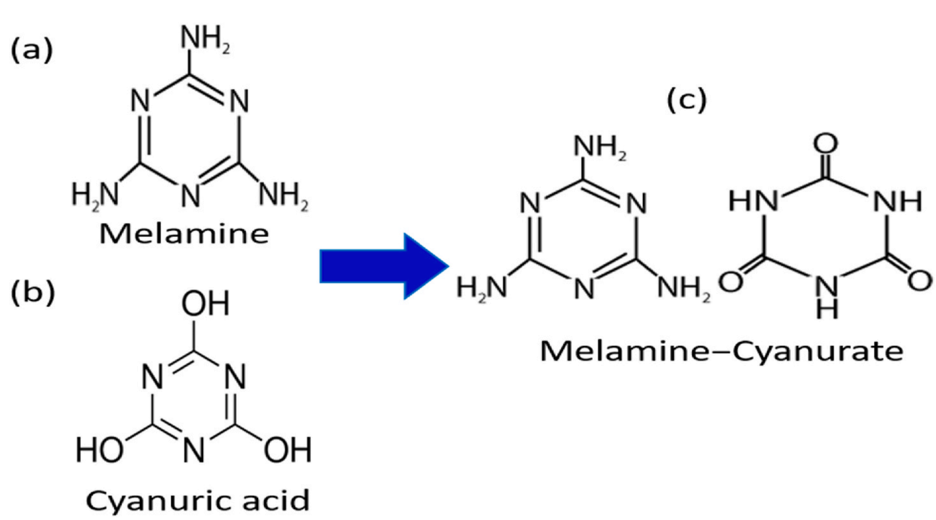

Fig. 1. Chemical structure of (a) melamine and (b) cyanuric acid and (c) melamine–cyanurate complex.

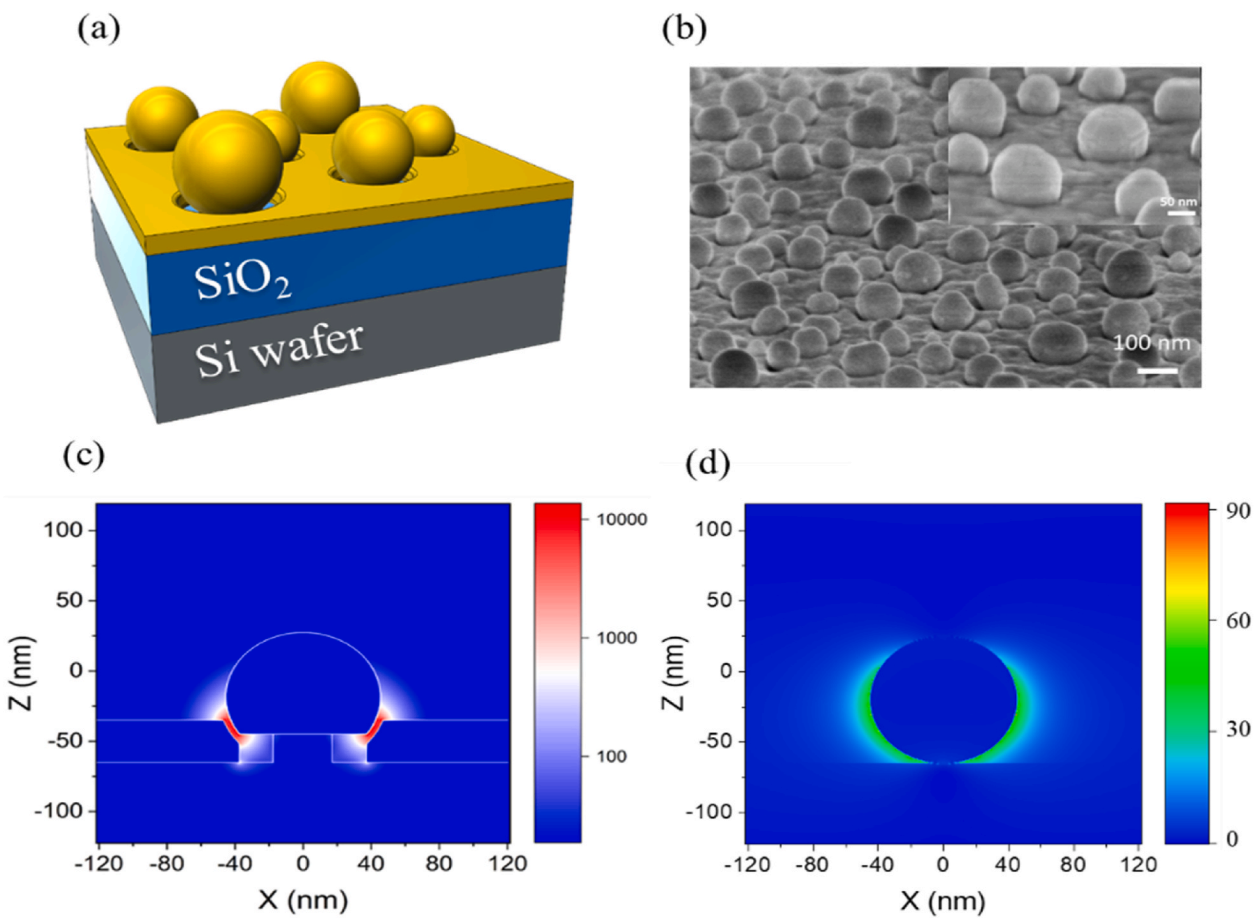

Fig. 2. (a) Schematic image of an Au nanogap sample. (b) Scanning electron microscope (SEM) image of an Au nanogap sample. (c) FDTD simulation result showing the enhancement of $|E|^2$ around the nanogap, where E is the electric field. (d) Electric field around gold nanosphere of size 90 nm on SiO_2 layer.

substrate that was capable of quantitative detection, with a high enhancement factor of 4.6×10^8. When averaged over four locations, the relative standard deviation (RSD) was 4.2% (Adhikari et al., 2022). Based on computations employing the FDTD (Finite-Difference Time-Domain) method, the electric field intensity ($|E|^2$) at the center of a 6 nm nanogap (90 nm diameter nanosphere) was found to be almost 60 times higher than that of a nanosphere with the same diameter but no gap arrangement (Fig. 2c) (Lumerical Inc.). Here, the fabrication of the SERS substrate at the optimal conditions for nanosphere diameter and nanogap allowed for the perfect matching of the localized surface plasmon resonance (LSPR) and Raman frequency, which is necessary for strong enhancement. As was previously documented, explosives like TNT, PETN, and RDX may be found down to the level of a single molecule (Adhikari et al., 2021), this augmented electromagnetic field in a small nanogap enhances the sensor performance ($\propto |E|^4$). The remarkable uniformity and high sensitivity of the used nanogap SERS substrates are essential for the quantitative identification of melamine and its byproducts in pet liquid food matrices (milk).

2.4. Raman measurements

A LabRAM HR-800 UV–Visible–NIR microscope (Horiba Jobin Yvon) with a multichannel air-cooled CCD detector was used to conduct the Raman scattering experiments. Approximately ~50 μW of incident power from a 785 nm laser served as the excitation source. For the SERS test, a 50× objective lens (N.A.:0.75) and a 10-s integration time were used. The SERS spectral data collection was carried out in the spectral range between 500 and 1620 cm^{-1} in order to identify the greatest amount of information about the melamine and cyanuric acid concentration without signal loss.

2.5. Data analysis

The raw SERS spectra were not fully acceptable during model construction due to the introduction of undesired effects that might reduce the effectiveness of prediction and classification models. The SERS data was preprocessed using a variety of methods, including range normalization, multiplicative signal correction (MSC), standard normal variate (SNV), and first and second Savitzky-Golay (SG) derivatives. The preprocessed data were then used to create a partial least-squares regression (PLSR) prediction analysis model, which was then compared using a hybrid linear analysis (HLA/GO). Furthermore, the suitable spectral bands required to improve prediction performance were extracted using a variable selection process (VIP). MATLAB (Version 7; Math Works, Natick, MA, USA) was used to do the entire spectrum study. *2.6. Classification analysis.*

In this study, a partial least squares discriminant analysis (PLS−DA) model was created to differentiate between various concentrations of each of the three chemical categories examined in pet liquid food (milk). This supervised classification technique is typically regarded as an altered version of the partial least squares regression (PLSR) technique (Barker and Rayens, 2003). In the PLS-DA model, the response variable Y contains binary values that represent different sample groups or categories. The following general form can be used to represent the PLS-DA equation:

$$Y = X \times b + E \tag{1}$$

X is the n × p matrix holding the SERS spectral data for each concentration sample, and b is the beta coefficient. E is the error matrix.

The spectrum data for both pure samples and pet liquid food samples that had been contaminated with harmful chemicals were found in matrix X of this study, whereas artificial values for each concentration were found in matrix Y. While developing the PLS-DA model, the entire spectrum data sets comprising 1750 samples (the ones infected with melamine) and 1500 samples (the ones infected with cyanuric acid and melamine combined with cyanuric acid). Two sets of data were separated from both datasets: a calibration set of 1400 samples and a validation set of 350 samples for melamine-contaminated samples. Of these, 1200 samples were transferred to the calibration set and the remaining 300 samples were used in the validation dataset for the remaining two categories. Additionally, a threshold of 0.5 was selected, implying that samples falling between the specified range will be categorized. There are three PLS-DA models created for every set of three sample groups.

2.6. Regression analysis

In this study, a popular machine learning algorithm called partial least-squares regression (PLSR) was used to analyze quantitatively the concentrations of melamine, cyanuric acid, and melamine combined with cyanuric acid present in pet liquid food (milk) samples. The prediction performance of PLSR was compared to another chemometric methodology called NAS regression-based hybrid linear analysis (HLA/GO). The following papers provide the mathematical aspects of NAS regression-based HLA/GO and PLSR (Bao and Dai, 2009; Goicoechea and Olivieri, 1999).

2.7. Waveband selection

Despite being highly significant, the large number of spectral wavebands in the spectrum data obtained with SERS contributed significantly to the elongation of the computing operation involved in analyzing the spectral data. Thus, choosing the right variables or waveband that enhanced the model's prediction accuracy and were closely related to the predictor variables was a crucial step in the waveband selection process. This study employed an application of frequently used powerful algorithm named as variable importance in projection (VIP) for the identification of key spectral wavebands for the enhancement of prediction performance of the multivariate analysis models. The variable's contribution to the description of the independent or spectral variables (X) and the dependent or reference data sets (Y) is determined by VIP. For more details, please refer the following article (Lohumi et al., 2015). In the past, several reports showed the strong potential of VIP algorithm to perform the non−destructive quantitative assessment of food and agricultural products (Joshi et al., 2023; Mohammadian et al., 2021). The VIP score of 0.85 was chosen as the ideal value in this study, and variables that were present below the threshold value were taken out of account. In order to improve prediction performance and taking less processing time, VIP was integrated with PLSR and SVR models during the creation of quantitative analysis models. The flowchart of the whole SERS spectrum data analysis of samples of spiked pet food (milk) in all three chemical categories is shown in Fig. 3.

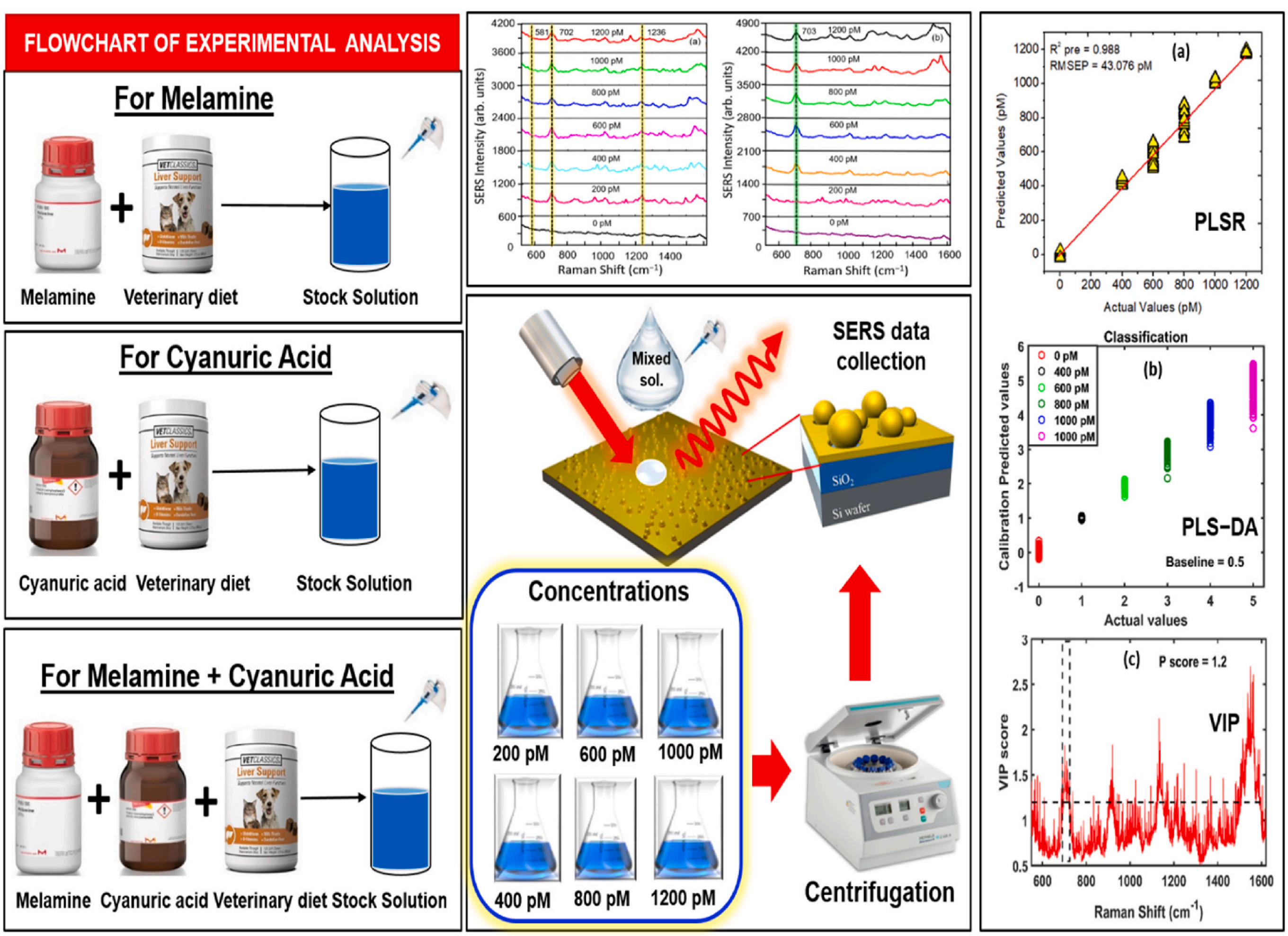

Fig. 3. A diagrammatic representation of the process used to process SERS spectral data for all three varieties of chemical-mixed pet liquid food.

2.8. Limit of detection (LOD)

The lowest concentration of an analyte in a sample that can be detected is the limit of detection. This parameter is used to assess the statistical significance of the quantitative analysis. For all three types of samples in this experiment, the LOD was calculated using Equation (2) in accordance with the International Committee on Harmonization (ICH) recommendations (Shrivastava and Gupta, 2011).

$$LOD = 3 \text{ x } S.D/C \quad (2)$$

where the term SD is defined as standard deviation, while c represents the slope of the regression line.

3. Results and discussions

3.1. Raw spectra for melamine, cyanuric acid, and melamine with cyanuric acid pet liquid food (milk)

Fig. S1 (a), (b), and (c) display the raw spectra of the three different types of samples: melamine mixed, cyanuric acid mixed, and melamine coupled with cyanuric acid mixed pet liquid food. The raw spectra, which typically consist of several overlapping peaks that undoubtedly depend on the noise generated by external factors, such as systematic noise, background, particle size, etc., suppress most of the useful information required for the identification of these chemicals in the pet liquid food samples selected for this research. The quality of the signal is directly and significantly impacted by this.

3.2. Spectral Interpretation for melamine, cyanuric acid, and melamine + cyanuric acid mixed pet liquid food

In this study, several different preprocessing steps, like normalization, MSC, SNV, and derivatives (Savitzky–Golay first and second), were implemented in the acquired raw spectra for all the three categories of samples with five distinct concentrations (200 pM, 400 pM, 600 pM, 800 pM, and 1200 pM), and the optimum preprocessing methods were selected based on the lowest root mean squares error values. The average preprocessed SERS spectra for the melamine-contaminated, cyanuric acid-contaminated, and melamine combined with cyanuric acid mixed pet liquid food (milk) samples were obtained using the Au nanogap substrate utilized in this work, and they are shown in Fig. 4a–c. The spectra were plotted from the 550–1610 cm^{-1} wavenumber range, while the uninformative spectral regions above 1610 and below 550 cm^{-1} were omitted in this investigation. The intensities of the spectral peaks for each of the three types of samples also rose progressively with the increment in the concentrations of chemicals on the samples. In our analysis, three distinct peaks at 581 (very low intensity), 702, and 1236 cm^{-1} were found for the melamine-contaminated samples in Fig. 4a. However, according to previously published research, the most noticeable spectrum peaks observed for melamine are at 703.5 cm^{-1} (Chong et al., 2013), 708 cm^{-1} (Tiwari et al., 2022), and 703 cm^{-1} (Cook et al., 2017) due to the triazine ring's breathing mode of vibration. Yet, during our investigation, the notable peak for melamine was found at 702 cm^{-1}, which is nearly identical and showed a minor shift of 1 cm^{-1}.

On the other hand, for the other two categories of samples i.e, cyanuric acid, and melamine combined with cyanuric acid identical concentrations were prepared in pet liquid food (milk)and further subjected to testing using SERS. The SERS spectra for cyanuric acid-spiked samples are depicted in Fig. 4b. The spectral peak for cyanuric acid, which was formed by ring out-of-plane bending vibration, was observed at 703 cm^{-1} in our study, while the peak was observed at 701.5 cm^{-1} in a published report (Chong et al., 2013). However, as the concentrations dropped from 1200 to 200 pM, the strength of the observed peak gradually decreased. As a result, cyanuric acid could be detected up to a 400 pM concentration range. For the melamine and cyanuric acid-spiked samples, the SERS spectra presnted in Fig. 4c demonstrate a spectral peak for melamine at 679 cm^{-1}, while the cyanuric peak shifted to a higher wavenumber range of 5 cm^{-1} and was observed at 708 cm^{-1}. Also, the spectral peaks intensities gradually decreased with the decrease in concentration. Therefore, the detection was also achievable up to a 400 pM concentration range in this category using the Au nanogap substrate used in this study. However, fewer additional spectral peaks were noticed at 1236 (due to Amide III (protein)) (Aitekenov et al., 2022) for melamine in Fig. 4a, while the SERS spectral peak in Fig. 4c at 988 cm^{-1} represents cyanuric acid, and the region from 1200 to 1300 cm^{-1} represents protein information (Aitekenov et al., 2022). Howeverthese peaks recieved little consideration and were likewise unable to make a major contribution to the identification of the main

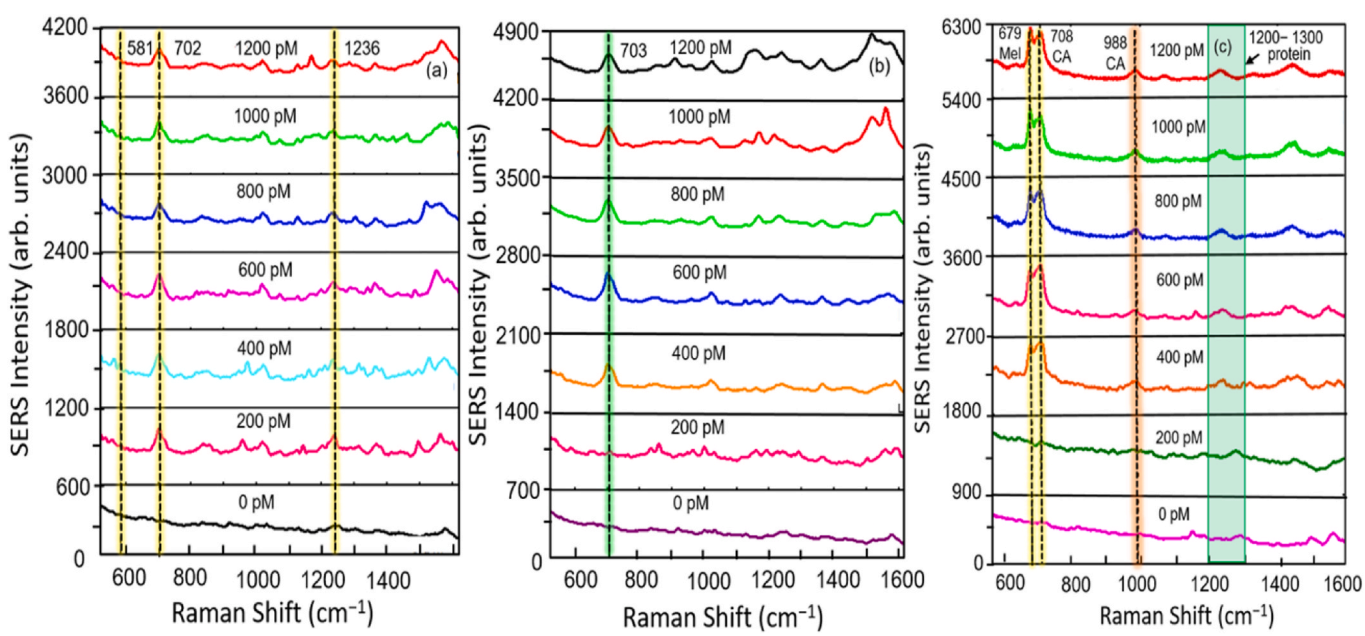

Fig. 4. SERS average preprocessed spectra for (a) melamine-contaminated, (b) cyanuric acid-contaminated, and (c) melamine combined with cyanuric acid-contaminated pet liquid food (milk) samples. The term 0 pM represents control samples or pure samples free from any contamination.

characteristics of the spectral features of melamine and cyanuric acid.

3.3. Dirichlet distribution algorithm

For all the three cases of samples in this study, 100 samples were measured, which is comparatively lower during model construction for machine learning and deep learning; this may result in underfitting. In this work, an algorithm developed by Dirichlet was used to address this problem. This algorithm's deep mathematical aspect has been described elsewhere (M. Wang et al., 2019). In the past, some researchers applied this technique to the assessment of phenolic compounds in Arabidopsis plants using IR, and NIR spectroscopy (Joshi et al., 2022), and moringa powder using FT-IR spectroscopy (Joshi et al., 2022). In total, 1750 synthetic samples were generated by the Dirichlet technique and used to build models afterward. Fig. 5 displays a broad overview of the Dirichlet algorithm for each of the three sample case scenarios. The spectra produced using two replicates for SERS data collection at position 5 and position 6 and represented as 200pM_1 and 200pM_5 are referred to here as the "original samples" in Fig. 5 (a), (c), and (e). However, in Fig. 5 (b, d, and f), the phrase "sample without noise" refers to the preprocessed spectra used to create artificial data.

3.4. PLS−DA classification model for melamine, cyanuric acid, and melamine combined with cyanuric acid samples

A supervised machine learning technique called partial least squares discriminant analysis (PLS-DA) was utilized to develop three classification models, one for each of the three data categories. The model developed for the melamine-spiked pet liquid food (milk) samples used a total of 1750 samples: 1400 for the calibration set and 350 for the validation dataset. Fig. 6a and b shows the classification plots for melamine-spiked samples, which used the SNV preprocessing strategy and obtained 100% overall accuracy. The remaining two sets of data (1200 for the calibration set and 300 for the validation set) totaled 1500 samples that were used for PLS-DA models. As seen in Fig. 6c and d, the Savitzky-Golay second preprocessing strategy produced classification plots of pet liquid food samples infected with cyanuric acid with an overall accuracy of 96%. Nevertheless, the third category of data yielded an overall accuracy of 95% when the Savitzky–Golay second preprocessing strategy was used. The classification plots for the calibration and validation sets are displayed in Fig. 6e and f, respectively. It can be concluded from the results that PLS-DA has the ability to qualitatively discriminate between pure and spiked pet liquid food samples when used in conjunction with appropriate preprocessing methods.

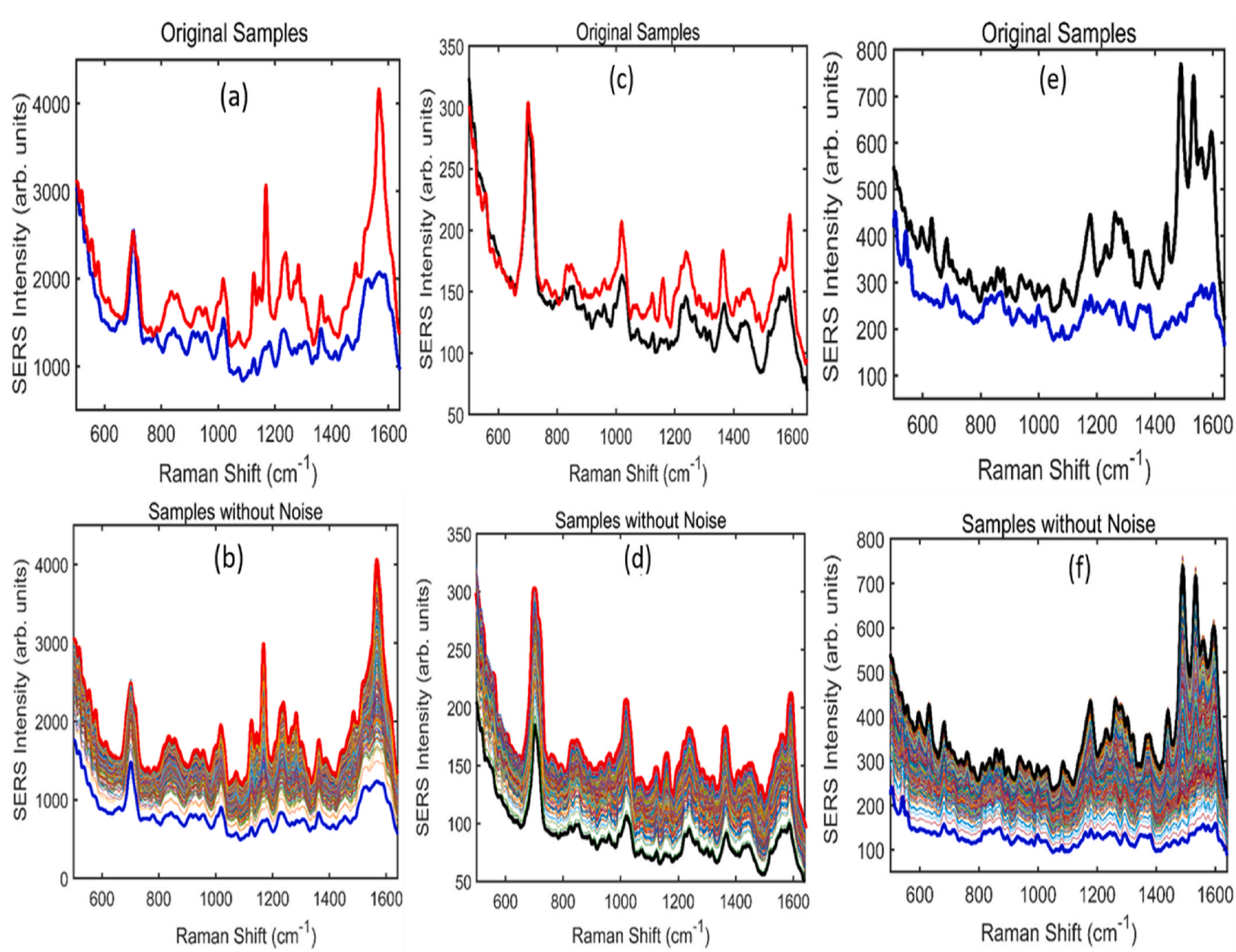

Fig. 5. SERS spectra generated among two replicates 200_1, and 200pM_5 for melamine, cyanuric acid, and combination of melamine + cyanuric acid (a, c, and e) using Dirichlet distribution. A total of 1750 artificial samples were created for SERS spectra for all the three categories using Dirichlet distribution (b, d, and f).

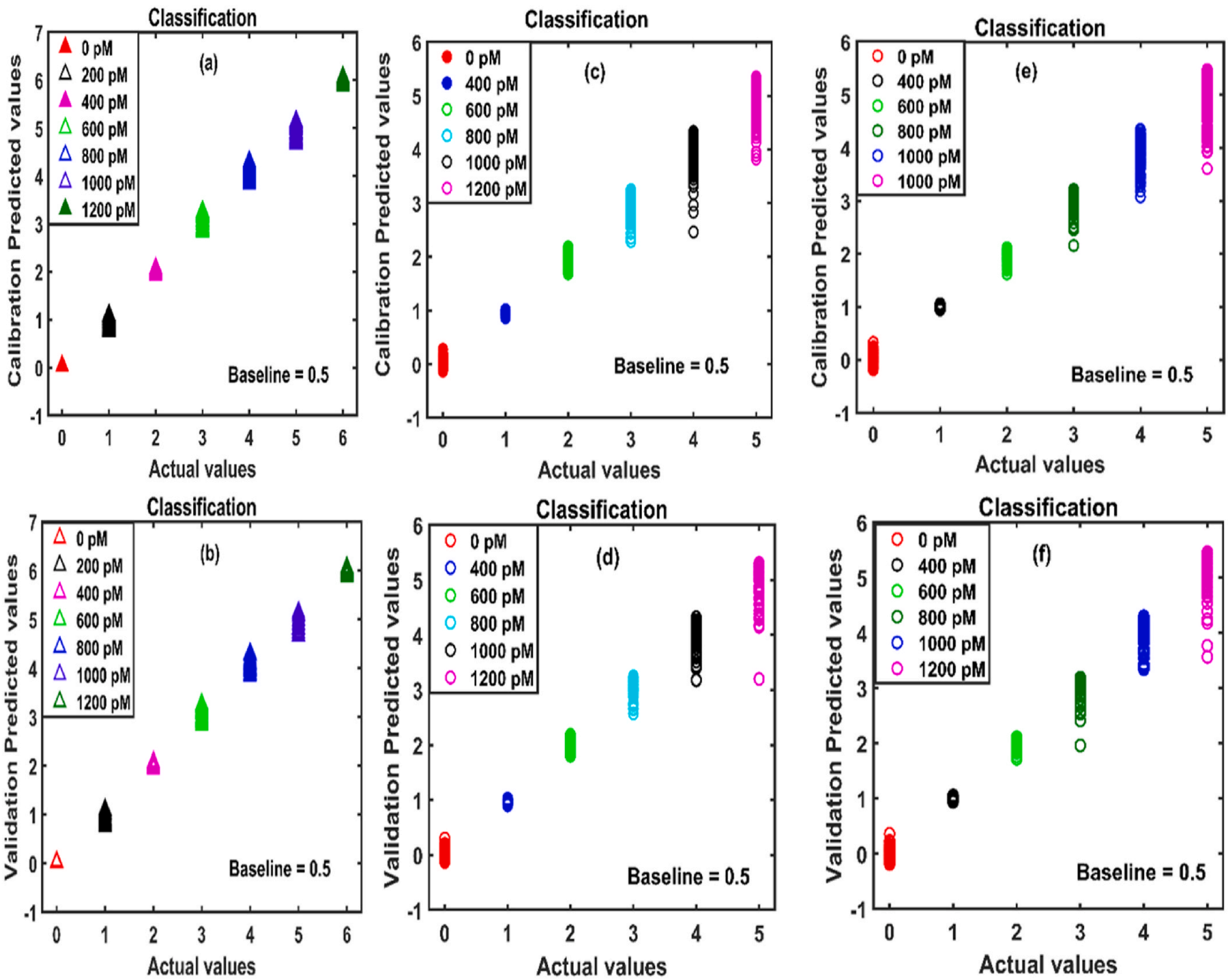

Fig. 6. PLS-DA classification plots for the following: (a, b) melamine spiked; (c, d) cyanuric acid spiked; and (e, f) melamine combined with cyanuric acid spiked pet liquid food samples.

3.5. Model development for the SERS spectral data

For the melamine-, cyanuric acid-, and combined chemical (melamine, cyanuric acid)-infected pet food (milk) samples, a quantitative prediction analytic model was built using PLSR regression. Since melamine contamination in pet liquid meals could be detected up to a 200 pM concentration range, 1750 samples were utilized in the model development process to produce calibration and prediction datasets. Although 400pM concentration levels were determined for the remaining two categories, 1500 samples were employed in the model's development, of which 1200 were used for calibration and 300 were added to the prediction datasets. In this work, the coefficient of determination (R^2), root mean square errors of calibration (RMSEC), prediction (RMSEP), and bias were chosen as crucial statistical metrics for the model evaluation. A model was regarded as superior if it had a high R^2 and lower values for errors and bias. Equation (3)−5 were utilized for the calculations of these statistical parameters' values in this study.

$$R^2 = \frac{\sum_{i=1}^{n} (y_i - \hat{y}_i)2}{\sum_{i=1}^{n} (y_i - \bar{y_i})2} \tag{3}$$

$$\text{RMSEP} = \sqrt{\frac{1 \sum_{i=1}^{n} (y_i - \hat{y}_i)2}{n}} \tag{4}$$

$$\text{Bias} = \frac{1}{n} \sum_{i=1}^{n} (y_i - \hat{y}_i) \tag{5}$$

where y_i and $\hat{y}_i$ are the actual and predicted chemical concentration values in pet liquid milk, respectively, and n is the number of predictions.

3.6. Prediction analysis results using PLSR for all three groups of samples

A PLSR model was first created for all three groups of samples in order to make a quantitative prediction. All three models underwent several preprocessing stages, as described in Section 2, from which the best preprocessing was chosen. For the melamine-infected samples, maximum normalization outperformed other preprocessing methods and yielded a higher correlation coefficient (R^2), with lower RMSE and bias values with the use of seven LVs selected based on the lower RMSE value. The results of the prediction study performed using the PLSR model for first group of samples are depicted in Fig. 7a and b. The results

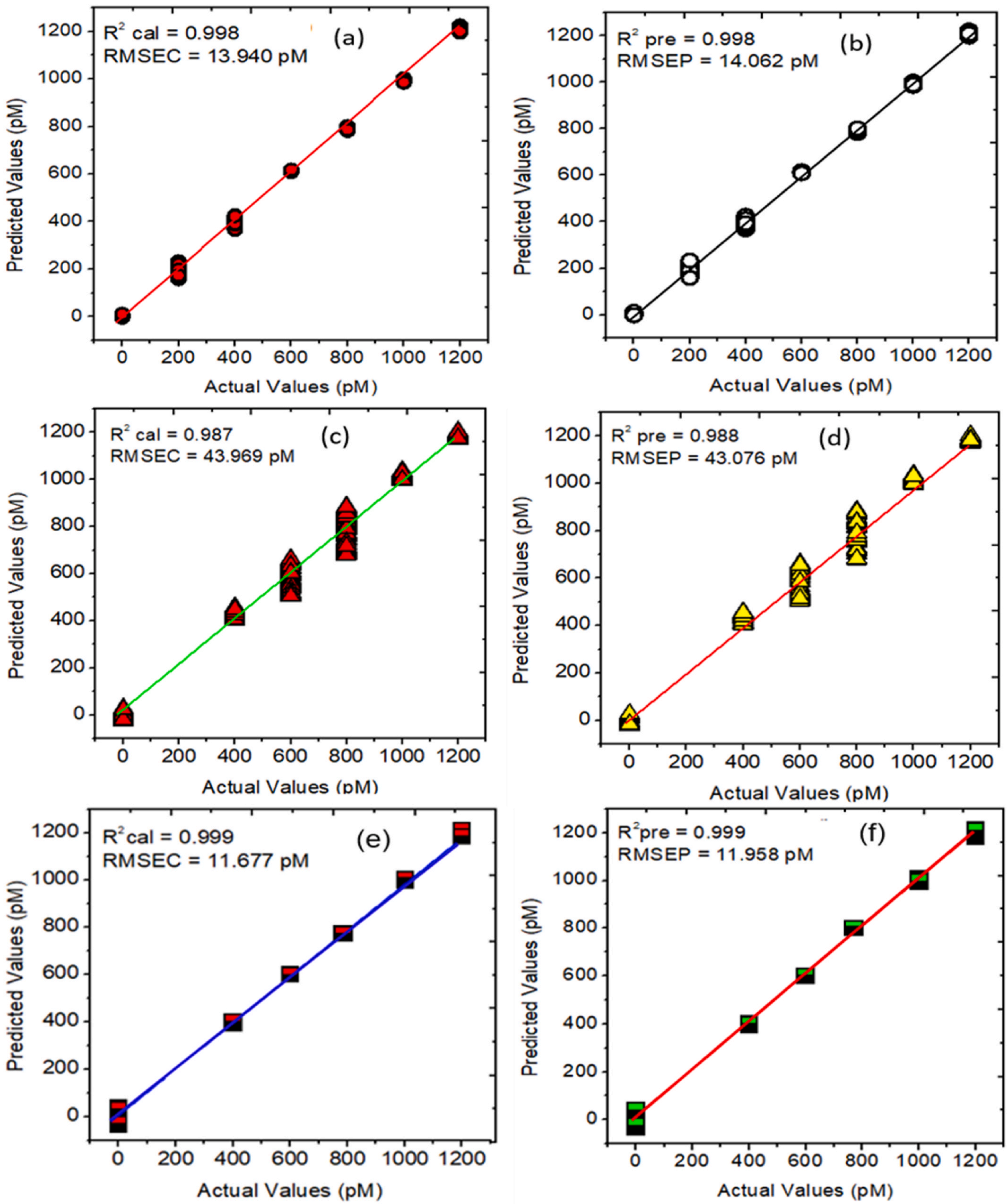

Fig. 7. Calibration and prediction plots for melamine-contaminated (a,b), cyanuric acid-contaminated (c,d), and melamine and cyanuric acid-contaminated pet liquid food (e, f) developed using the PLSR model.

display a linear relationship between the actual and predicted concentration values, and detection was achieved until 200 pM. For the calibration set, the model produced an R^2 value of 0.998 and an RMSEC value of 13.940 pM. Although the R^2 values for the higher prediction sets were similar (0.998), the RMSEP error value was larger (14.062 pM). On the other hand, the PLSR model for second contaminated group of samples produced an R^2 values of 0.987 and 0.988, with RMSE values of 43.969 and 43.076 for both the calibration and prediction datasets, respectively shown in Fig. 7c and d. The relationship between the actual and predicted concentration values was also linear in this case, but detection was achieved up to 400 pM due to the absence of a spectral peak for cyanuric acid in 200 pM solution concentrations as shown in Fig. 4b. With the use of four LVs, mean normalization performed better as a preprocessing strategy in this group of samples. Additionally, for third group of contaminated samples, the calibration and prediction datasets delivered an R^2 value of 0.999 with lower RMSE values of 11.677 and 11.958 pM than the other two previously developed regression models as illustrated on Fig. 7e and f. However, the maximum detection of these combined chemicals was accomplished up to 400 p.m. due to absence of spectral peaks in Fig. 4c. Table 1 displays the entire prediction analysis results acquired using the PLSR models for all three categories of samples. Hybrid linear analysis (HLA/GO) based on NAS regression was used to compare the prediction performance of PLSR. Table 1 presents the results of the prediction analysis. It is evident from this that the developed PLSR model outperformed the HLA/GO model in terms of prediction errors values, as evidenced by the poor root mean square error of prediction for all three categories of samples obtained using HLA/GO models.

3.7. Regression coefficients for the constructed PLSR model for all three groups of samples

For the purpose of identifying significant spectrum regions that were directly related to the chemical characteristics of molecules, regression or beta coefficients plots were of greatest significance. In this study, beta coefficients plots were produced for each of the three cases of contaminated pet liquid food samples using the established PLSR models. A beta coefficient plot for the melamine-contaminated samples is shown in Fig. S2a. These samples showed spectral signatures for melamine at 702 cm^{-1} due to triazine ring's breathing mode of vibration and for protein (Amid III) at 1200–1300 cm^{-1}, which were both the same as the average spectra for melamine that were previously shown in Fig. 4a and marked with arrow and rectangle box. Similar beta coefficients plots were produced using the PLSR models for the other two categories of contaminated samples, as shown in Fig. S2 b, c. According to Fig. 4b and c, both plots produced identical spectral peaks that were sensitive to the harmful chemicals in pet meals, suggesting that beta coefficient plots were an important tool for finding characteristic spectrum wavelengths.

3.8. Quantitative model development using VIP waveband selection

A waveband selection technique known as VIP was added to the three PLSR models that had already been developed in order to improve prediction performance and identify key spectral waveband regions that are sensitive to additional chemicals in pet liquid foods. This was done because the PLSR model had a higher prediction performance as discussed in section 3.6. Several values for the VIP score were used, and throughout the VIP waveband selection process, an optimum value of 1.2 was chosen. Following this procedure, PLSR models were constructed using the obtained waveband regions for each of the three sample groups. The number of variables, or wavenumbers, for the reference solution, mango juice, and milk samples were lowered from 2040 to 396, 428, and 422 following the completion of the VIP analysis. For each of the three categories of data, the following pre-selected variables were used to generate the PLSR model. Then, the performance of that model was compared with the performance of the PLSR model that included all 2040 variables. The prediction performance outcomes for the chosen variables that were produced using VIP are displayed in Table 2 alongside the total set of variables. For the standard solution, mango juice, and milk prediction datasets, the coefficient of determination (R^2) values were 0.999, 0.985, and 0.981, respectively. These results were nearly indistinguishable from the whole PLSR model with a bias values of 1.369, −1.426, and 0.999.

Furthermore, the VIP score graphs associated to cyanuric acid and melamine are displayed in Fig. 8, together with sensitive spectral wavelength areas. The VIP score plot in Fig. 8a illustrates the spectra of the melamine-spiked pet liquid food samples. The regions marked in red with the rectangle box represent similar spectral peaks as those reported in Fig. 4a in Section 3.2. Similarly, for other remaining two categories, the VIP score plots in Fig. 8b and c displays sensitive spectral signatures for cyanuric acid and melamine mixed with cyanuric acid which are identical with that mentioned in Fig. 4b and c in Section 3.2 and highlighted with rectangular boxes. Even though the VIP-PLSR model's prediction dataset has higher RMSEP error values than the PLSR model's, the former model was crucial in identifying important spectral signatures by removing undesired variables, which also had an immediate impact on the amount of computational time required for the analysis when designing any industrial applications. It may thus be concluded that the VIP-PLSR model outperforms the PLSR model with all variables in terms of processing speed and important waveband region identification.

3.9. Model validation

A new variety of pet liquid food (milk) was purchased, and similar six different concentrations, including the pure milk mentioned in Section 2.2, were prepared for melamine-, cyanuric acid-, and melamine combined with cyanuric acid-contaminated milk samples. This was done to ensure the applicability of the developed VIP−PLSR models for all three groups of contaminated samples. The average preprocessed SERS spectra for melamine, cyanuric acid, and melamine and cyanuric acid contaminated samples are shown in Fig. 9a–c. The distinctive spectral SERS peak is visible in the melamine-contaminated SERS spectra in Fig. 9a and is comparable to that in Fig. 4a. As the concentration was reduced to 200 pM, the intensity of this peak steadily decreased. The detection, however, was successful up to a 200 pM concentration range. The SERS spectral peak for cyanuric acid at 702.455 cm^{-1}, the peak for melamine at 680 cm^{-1}, and the peak for cyanuric acid at 707 cm^{-1} exhibited in Fig. 9b and c was all in good agreement with the peak first identified in Fig. 4b and c, and detection was successful up to the 400 pM

Table 1
Prediction analysis findings achieved through the PLSR model for all three group of samples.

Region	Samples	Model/Preprocessing	R_c^2	RMSEC (pM)	R_p^2	RMSEP (pM)	LVs	bias
SERS spectroscopy	Melamine + pet liquid food	PLSR/Max. norm.	0.998	13.940	0.998	14.062	7	−0.665
		HLA/GO/Range norm.	0.985	18.972	0.991	20.123	6	0.702
	Cyanuric acid + pet liquid food	PLSR/Mean norm.	0.997	18.095	0.998	16.677	5	0.791
		HLA/GO/MSC	0.992	20.123	0.985	21.001	8	0.878
	Melamine + Cyanuric acid + pet liquid food	PLSR/Mean norm.	0.999	11.677	0.999	11.958	6	−0.555
		HLA/GO/SNV	0.957	21.252	0.961	20.125	7	0.997

Table 2
Prediction analysis findings achieved through the PLSR and VIP−PLSR model for all three group of samples.

Samples	Models/Preprocessing	R_c^2	RMSEC (pM)	R_p^2	RMSEP (pM)	LVs	bias
Melamine + pet liquid food	PLSR/Max. norm.	0.998	13.940	0.998	14.062	7/2040	−0.665
	VIP−PLSR/Max. norm.	0.997	19.388	0.997	18.492	6/396	1.369
Cyanuric acid + pet liquid food	PLSR/Mean norm.	0.997	18.095	0.998	16.677	5/2040	−0.791
	VIP−PLSR/Mean norm.	0.992	18.874	0.985	19.777	8/428	−1.426
Melamine + Cyanuric acid + pet liquid food	PLSR/Mean norm.	0.999	11.677	0.999	11.958	6/2040	−0.555
	VIP−PLSR/ Mean norm.	0.980	16.021	0.981	15.124	7/422	0.990

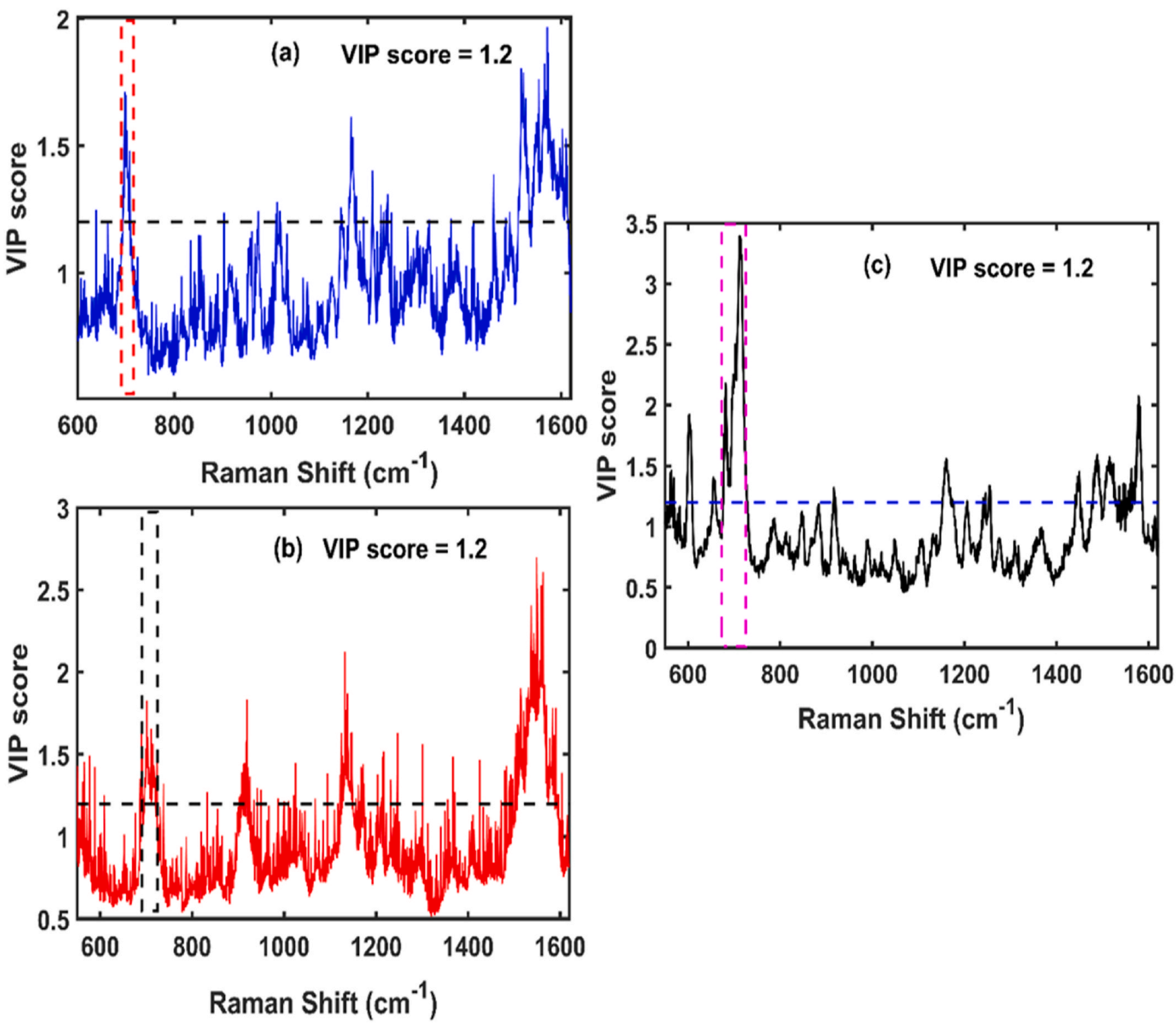

Fig. 8. VIP score diagrams for the following three scenarios: (a) melamine, (b) cyanuric acid, and (c) melamine combined with cyanuric acid spiked pet liquid food samples (a). The rectangular dashed box indicates the key wavenumber regions that were selected using VIP and are prone to added chemicals.

concentration range.

To further confirm how the previously constructed model works for different types of pet liquid food (milk) samples, similar PLSR models to those developed in Section 3.5 were employed for each of the three sets of samples in this case. The model outcomes for the melamine-contaminated samples are shown in Fig. 10a. The result had a greater corelation coefficient (R^2) of 0.999 for both the calibration and prediction datasets with lower RMSEC and RMSEP values of 10.495, and 10.501 pM, respectively. On the other hand, Fig. 10b and c presents the obtained results for the final two sample groups. The model performed well in both of these categories, achieving greater R^2 and lower RMSEC and RMSEP error rates, as well as a higher correlation coefficient. The final results for the PLSR models for each of the three types of samples are presented in Table 3.

The obtained results clearly show that the SERS Au nanogap substrate has a high potential for the fast and efficient detection of melamine, cyanuric acid, and their combined form at concentrations as low as picomolar in pet liquid food samples when combined with VIP−PLSR

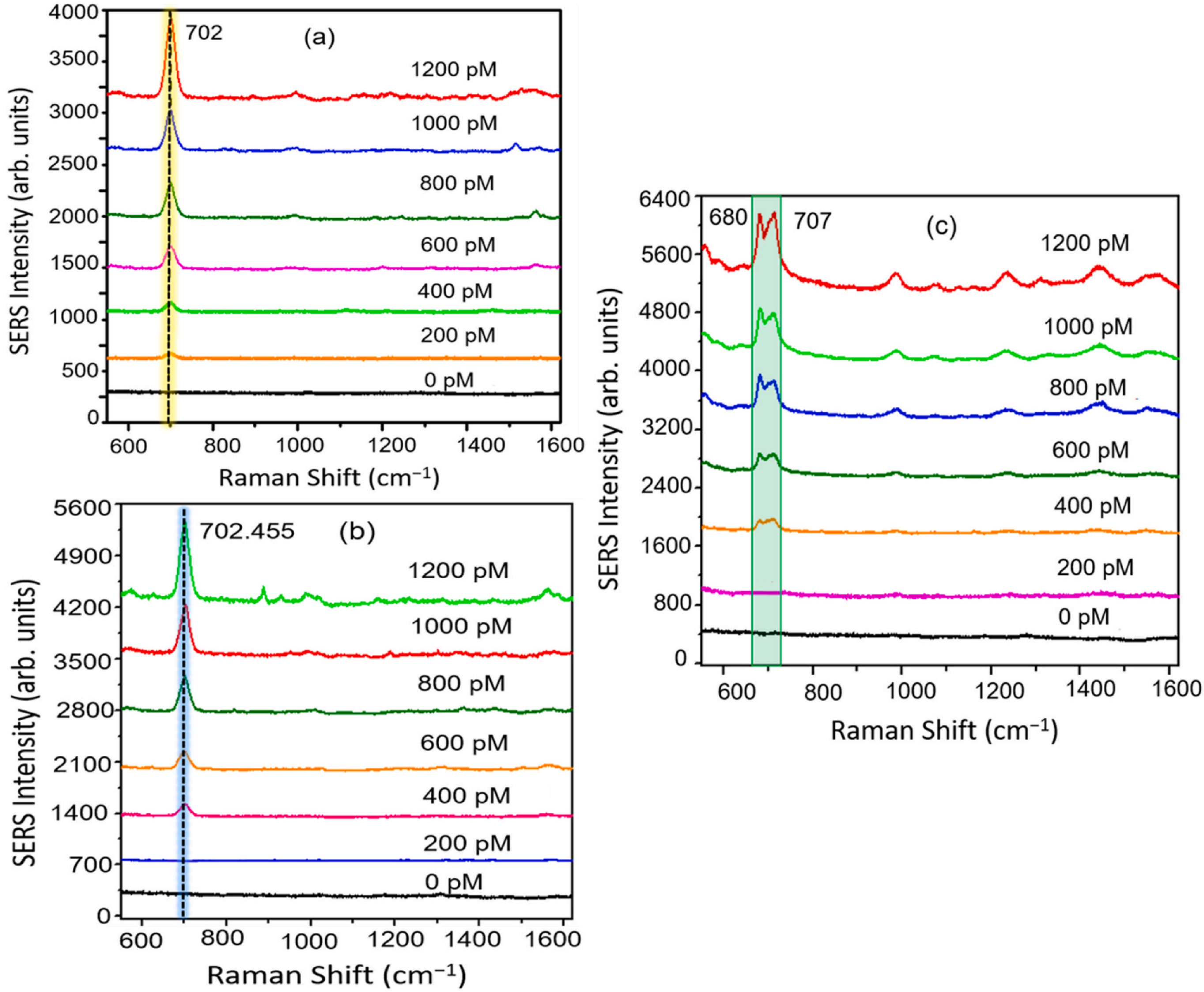

Fig. 9. SERS average preprocessed spectra for (a) melamine-contaminated, (b) cyanuric acid-contaminated, and (c) melamine combined with cyanuric acid-contaminated pet liquid food (milk) for a new variety of sample.

(partial least-squares regression) and suitable preprocessing techniques. Additionally, the new method unequivocally shown that, in comparison to conventional spectroscopies and imaging approaches, the SERS Au nanogap substrate offers greater detection capabilities. In a prior study, cyanuric acid and melamine in milk were detected using a SERS gold substrate with an R^2 of 0.90 (Liu et al., 2010). These two dangerous chemicals were, nonetheless, detected in milk up to a quantity of 2 ppm according to this investigation. In a different investigation, melamine in milk up to 0.5 ppm was detected using SERS in combination with an Ag nanocube array substrate (Li and Chin, 2021). Both of these results, however, are completely unreliable if the relevant dangerous compounds are present in amounts lower than 0.5 ppm. The limitation of previous research on low concentration detection was overcome by our study, which was able to achieve a stronger detection capacity by using the SERS Au nanogap substrate in this inspection. Further, GC/MS (Pan et al., 2013) and LC/MS (Turnipseed et al., 2008) methods have been used to detect melamine and cyanuric acid in food products, including dairy products, although these two approaches are highly sensitive and offer detection up to ng levels. Nevertheless, SERS offers other advantages, such as simple sample preparation, quick detection, and the absence of complex instrumentation needed for sample measurements. We further addressed the shortcomings of these methods in our study by using more samples in the model analysis and achieving the lowest RMSE errors and a higher correlation coefficient (R^2) for each of the three categories of data. So, based on the results obtained, it could therefore be concluded that the SERS Au nanogap substrate in conjunction with the VIP-based partial least squares regression (PLSR) model could replace time-consuming, destructive procedures for the quantitative analysis of melamine and cyanuric acid in pet liquid food (milk) samples. This research will be extended in the future to detect additional hazardous chemical additives that may be present in different kinds of pet food matrices.

4. Conclusions

In the present investigation, melamine, cyanuric acid, and melamine coupled with cyanuric acid were identified in pet liquid food (milk) samples using a SERS Au nanogap substrate. With RMSEP values of 14.062, 16.677, and 11.958 pM, respectively, the PLSR machine learning model earned the highest correlation coefficients (R^2) of 0.998, 0.998, and 0.999 in contrast to the NAS-based HLA/GO model. Additionally, the three sets of infected pet liquid food (milk) samples had

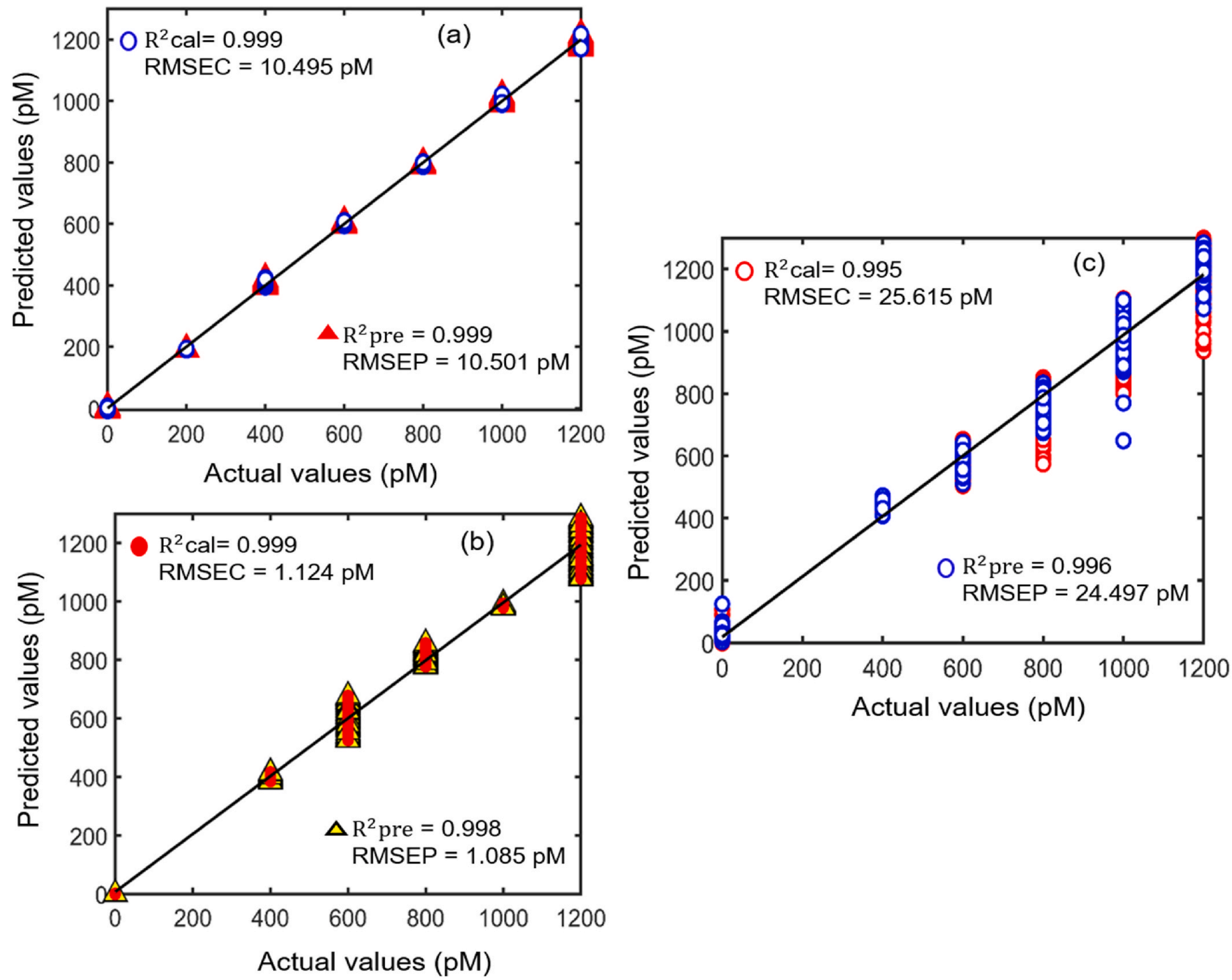

Fig. 10. Calibration and Prediction plots for melamine contaminated (a), cyanuric acid contaminated (b), and melamine combined with cyanuric acid contaminated pet liquid food (c) developed using PLSR model. Here the terms R^2cal: correlation coefficient for calibration; R^2pre: correlation coefficient for prediction; RMSEC: root mean square of calibration; RMSEP: root mean square of prediction; PLSR: partial least squares regression.

Table 3
Prediction analysis findings achieved through VIP−PLSR model for all the three group of samples.

Region	Samples	R_c^2	RMSEC (pM)	R_p^2	RMSEP (pM)	LVs	bias
SERS spectroscopy	Melamine + pet liquid food	0.999	10.495	0.999	10.501	7	−0.796
	Cyanuric acid + pet liquid food	0.999	1.124	0.998	1.085	6	−0.0132
	Melamine + Cyanuric acid + pet liquid food	0.995	25.615	0.996	24.497	5	1.624

good LOD values of 0.40, 0.42, and 0.31 pM due to the Au nanogap substrate's higher sensitivity, homogeneity, and enhancement factors. VIP score plots were also utilized to improve prediction accuracy by identifying significant spectral signatures that were responsive to the additional compounds in pet food matrices. The constructed PLSR models were used with a waveband selection technique to exclude unwanted spectral waveband areas. Our model performance findings were confirmed by utilizing more food-related data, which resulted in lower RMSEP values and a higher R^2 values. Furthermore, PLS-DA showed the highest classification accuracy of 100%, 96%, and 95% for all three categories of added chemicals, demonstrating its ability to distinguish between pure and spiked samples. The findings unambiguously demonstrated that the SERS Au nanogap substrate, when used in conjunction with the VIP−PLSR machine learning method, could serve as an effective replacement for conventional spectroscopic and destructive chemical analysis techniques. It could also offer a rapid and efficient quantitative assessment of melamine and its byproducts in liquid meals intended for animal consumption.

CRediT authorship contribution statement

Rahul Joshi: Conceptualization, Methodology, Formal analysis, Writing – original draft. **Samir Adhikari:** Methodology, Conceptualization, Formal analysis. **Minjun Kim:** Methodology. **Yudong Jang:** Conceptualization, Methodology. **Hyun Jung Min:** Methodology. **Donghan Lee:** Conceptualization, Methodology, Formal analysis, Writing – review & editing, Project administration. **Byoung-Kwan Cho:** Conceptualization, Methodology, Formal analysis, Writing – review &

editing, Project administration, Resources, Supervision.

Declaration of competing interest

The authors declare that they have no known competing financial interests or personal relationships that could have appeared to influence the work reported in this paper.

Data availability

Data will be made available on request.

Acknowledgments

The authors also acknowledge supports from the National Research Foundation of Korea (grant numbers 2017R1A6A3A11031648, 2019R1I1A3A01057628, 2020R1A6A1A03047771, and 2021R1I1A1A01040695), by Chungnam National University (CNU), and BK21 FOUR Project for Smart Agriculture Systems, Chungnam National University, Republic of Korea.

Appendix A. Supplementary data

Supplementary data to this article can be found online at https://doi.org/10.1016/j.crfs.2024.100726.

References

Abbas, O., Lecler, B., Dardenne, P., Baeten, V., 2013. Detection of melamine and cyanuric acid in feed ingredients by near infrared spectroscopy and chemometrics. J. Near Infrared Spectrosc. 21 (3), 183–194. https://doi.org/10.1255/jnirs.1047.

Adhikari, S., Ampadu, E.K., Kim, M., Noh, D., Oh, E., Lee, D., 2021. Detection of explosives by SERS platform using metal nanogap substrates. Sensors 21 (16). https://doi.org/10.3390/s21165567.

Adhikari, S., Kim, M., Lee, J., Jang, Y., Lee, D., 2022. A new approach to quantitative SERS with high sensitivity: vertical gap control. Biophotonics in Point-of-Care II. PC1214506.

Aitekenov, S., Sultangaziyev, A., Ilyas, A., Dyussupova, A., Boranova, A., Gaipov, A., Bukasov, R., 2022. Surface-enhanced Raman spectroscopy (SERS) for protein determination in human urine. Sens. Bio-Sens. Res. 38 (October), 100535 https://doi.org/10.1016/j.sbsr.2022.100535.

Bao, X., Dai, L., 2009. Partial least squares with outlier detection in spectral analysis: a tool to predict gasoline properties. Fuel 88 (7), 1216–1222. https://doi.org/10.1016/j.fuel.2008.11.025.

Barker, M., Rayens, W., 2003. Partial least squares for discrimination. J. Chemometr. 17 (3), 166–173. https://doi.org/10.1002/cem.785.

Bielejewska, A.G., Marjo, C.E., Prins, L.J., Timmerman, P., De Jong, F., Reinhoudt, D.N., 2001. Thermodynamic stabilities of linear and crinkled tapes and cyclic rosettes in melamine-cyanurate assemblies: a model description. J. Am. Chem. Soc. 123 (31), 7518–7533. https://doi.org/10.1021/ja010664o.

Chen, Z., Yan, X., 2009. Simultaneous determination of melamine and 5-hydroxymethylfurfural in milk by capillary electrophoresis with diode array detection. J. Agric. Food Chem. 57 (19), 8742–8747. https://doi.org/10.1021/jf9021916.

Chong, N.S., Smith, K.A., Setti, S., Ooi, B.G., 2013. Application of gold and silver colloidal nanoparticles for the surface-enhanced Raman spectrometric analysis of melamine and 4-aminobiphenyl. Int. J. Environ. Technol. Manag. 16 (1–2), 3–20. https://doi.org/10.1504/IJETM.2013.050681.

Cook, A.L., Carson, C.S., Marvinney, C.E., Giorgio, T.D., Mu, R.R., 2017. Sensing trace levels of molecular species in solution via zinc oxide nanoprobe Raman spectroscopy. J. Raman Spectrosc. 48 (8), 1116–1121. https://doi.org/10.1002/jrs.5180.

De Lourdes Mendes Finete, V., Gouvêa, M.M., De Carvalho Marques, F.F., Netto, A.D.P., 2013. Is it possible to screen for milk or whey protein adulteration with melamine, urea and ammonium sulphate, combining Kjeldahl and classical spectrophotometric methods? Food Chem. 141 (4), 3649–3655. https://doi.org/10.1016/j.foodchem.2013.06.046.

Dorne, J. Lou, Doerge, D.R., Vandenbroeck, M., Fink-Gremmels, J., Mennes, W., Knutsen, H.K., Vernazza, F., Castle, L., Edler, L., Benford, D., 2013. Recent advances in the risk assessment of melamine and cyanuric acid in animal feed. Toxicol. Appl. Pharmacol. 270 (3), 218–229. https://doi.org/10.1016/j.taap.2012.01.012.

Fan, Y., Lai, K., Rasco, B.A., Huang, Y., 2015. Determination of carbaryl pesticide in Fuji apples using surface-enhanced Raman spectroscopy coupled with multivariate analysis. Lwt 60 (1), 352–357. https://doi.org/10.1016/j.lwt.2014.08.011.

Filazi, A., Sireli, U.T., Ekici, H., Can, H.Y., Karagoz, A., 2012. Determination of melamine in milk and dairy products by high performance liquid chromatography. J. Dairy Sci. 95 (2), 602–608. https://doi.org/10.3168/jds.2011-4926.

Fleischmann, M., Hendra, P.J., McQuillan, A.J., 1974. Raman spectra of pyridine adsorbed at a silver electrode. Chem. Phys. Lett. 26 (2), 163–166.

Goicoechea, H.C., Olivieri, A.C., 1999. Wavelength selection by net analyte signals calculated with multivariate factor-based hybrid linear analysis (HLA). A theoretical and experimental comparison with partial least-squares (PLS). Analyst 124 (5), 725–731. https://doi.org/10.1039/a900325h.

Joshi, R., Adhikari, S., Pil Son, J., Jang, Y., Lee, D., Cho, B.K., 2023. Au nanogap SERS substrate for the carbaryl pesticide determination in juice and milk using chemomterics. Spectrochim. Acta Mol. Biomol. Spectrosc. 297 (April), 122734 https://doi.org/10.1016/j.saa.2023.122734.

Joshi, R., Sathasivam, R., Jayapal, P.K., Patel, A.K., Van Nguyen, B., Faqeerzada, M.A., Park, S.U., Lee, S.H., Kim, M.S., Baek, I., Cho, B.K., 2022a. Comparative determination of phenolic compounds in Arabidopsis thaliana leaf powder under distinct stress conditions using fourier-transform infrared (FT-IR) and near-infrared (FT-NIR) spectroscopy. Plants 11 (7). https://doi.org/10.3390/plants11070836.

Joshi, R., Sathasivam, R., Park, S.U., Lee, H., Kim, M.S., Baek, I., 2022b. Application of Fourier Transform Infrared Spectroscopy and Multivariate Analysis Methods for the Non-destructive Evaluation of Phenolics Compounds in Moringa Powder, pp. 1–17.

Kuo, F.C., Tseng, Y.T., Wu, S.R., Wu, M.T., Lo, Y.C., 2013. Melamine activates NFκB/COX-2/PGE2 pathway and increases NADPH oxidase-dependent ROS production in macrophages and human embryonic kidney cells. Toxicol. Vitro 27 (6), 1603–1611. https://doi.org/10.1016/j.tiv.2013.04.011.

Li, L., Chin, W.S., 2021. Rapid and sensitive SERS detection of melamine in milk using Ag nanocube array substrate coupled with multivariate analysis. Food Chem. 357 (March), 129717 https://doi.org/10.1016/j.foodchem.2021.129717.

Liu, B., Lin, M., Li, H., 2010. Potential of SERS for rapid detection of melamine and cyanuric acid extracted from milk. Sens. Instrument. Food Qual. Saf. 4 (1), 13–19. https://doi.org/10.1007/s11694-009-9091-3.

Lohumi, S., Lee, S., Cho, B.K., 2015. Optimal variable selection for Fourier transform infrared spectroscopic analysis of starch-adulterated garlic powder. Sens. Actuators, B 216, 622–628. https://doi.org/10.1016/j.snb.2015.04.060.

Miao, H., Fan, S., Wu, Y.N., Zhang, L., Zhou, P.P., Li, J.G., Chen, H.J., Zhao, Y.F., 2009. Simultaneous determination of melamine, ammelide, ammeline, and cyanuric acid in milk and milk products by gas chromatography-tandem mass spectrometry. Biomed. Environ. Sci. 22 (2), 87–94. https://doi.org/10.1016/S0895-3988(09)60027-1.

Mohammadian, A., Barzegar, M., Mani-Varnosfaderani, A., 2021. Detection of fraud in lime juice using pattern recognition techniques and FT-IR spectroscopy. Food Sci. Nutr. 9 (6), 3026–3038. https://doi.org/10.1002/fsn3.2260.

Pan, X.D., Wu, P. gu, Yang, D.J., Wang, L.Y., Shen, X.H., Zhu, C.Y., 2013. Simultaneous determination of melamine and cyanuric acid in dairy products by mixed-mode solid phase extraction and GC-MS. Food Control 30 (2), 545–548. https://doi.org/10.1016/j.foodcont.2012.06.045.

Patel, K., Jones, K., 2007. Analytical method for the quantitative determination of cyanuric acid as the degradation product of sodium dichloroisocyanurate in urine by liquid chromatography mass spectrometry. J. Chromatogr., B: Anal. Technol. Biomed. Life Sci. 853 (1–2), 360–363. https://doi.org/10.1016/j.jchromb.2007.03.014.

Ranganathan, A., Pedireddi, V.R., Rao, C.N.R., Box, J.P.O., Recei, V., No, V., 1999. Hydrothermal Synthesis of Organic Channel Structures : 1 : 1 Hydrogen-Bonded Adducts of Melamine with Cyanuric and Trithiocyanuric Acids Chemistry & Physics of Materials Unit Jawaharlal Nehru Centre for Ad V Anced Scientific Research (M) -forming Rosett, vol. 8, pp. 1752–1753.

Rovina, K., Siddiquee, S., 2015. A review of recent advances in melamine detection techniques. J. Food Compos. Anal. 43, 25–38. https://doi.org/10.1016/j.jfca.2015.04.008.

Shrivastava, A., Gupta, V., 2011. Methods for the determination of limit of detection and limit of quantitation of the analytical methods. Chronicles Young Sci. 2 (1), 21. https://doi.org/10.4103/2229-5186.79345.

Stine, C.B., Reimschuessel, R., Keltner, Z., Nochetto, C.B., Black, T., Olejnik, N., Scott, M., Bandele, O., Nemser, S.M., Tkachenko, A., Evans, E.R., Crosby, T.C., Ceric, O., Ferguson, M., Yakes, B.J., Sprando, R., 2014. Reproductive toxicity in rats with crystal nephropathy following high doses of oral melamine or cyanuric acid. Food Chem. Toxicol. 68, 142–153. https://doi.org/10.1016/j.fct.2014.02.029.

Su, X., Zhou, H.Y., Chen, F.C., Gao, B.X., Liu, Z.W., Zhang, Y.H., Liu, F., Liu, F., Li, Z.R., Gao, Z.X., 2013. Modified SBA-15 matrices for high-throughput screening of melamine in milk samples by MALDI-TOF MS. Int. J. Mass Spectrom. 338, 39–44. https://doi.org/10.1016/j.ijms.2012.11.006.

Tiwari, M., Singh, A., Thakur, D., Pattanayek, S.K., 2022. Graphitic carbon nitride-based concoction for detection of melamine and R6G using surface-enhanced Raman scattering. Carbon 197 (April), 311–323. https://doi.org/10.1016/j.carbon.2022.06.035.

Turnipseed, S., Casey, C., Nochetto, C., Heller, D.N., 2008. Determination of melamine and cyanuric acid residues in infant formula using LC-MS/MS. Lab. Inform. Bullet. 4421, 496–549.

Wang, M., Zhao, M., Chen, J., Rahardja, S., 2019. Nonlinear unmixing of hyperspectral data via deep autoencoder networks. Geosci. Rem. Sens. Lett. IEEE 16 (9), 1467–1471. https://doi.org/10.1109/lgrs.2019.2900733.

Wang, P., Pang, S., Chen, J., McLandsborough, L., Nugen, S.R., Fan, M., He, L., 2016. Label-free mapping of single bacterial cells using surface-enhanced Raman spectroscopy. Analyst 141 (4), 1356–1362. https://doi.org/10.1039/c5an02175h.

Yilmaz, H., Culha, M., 2022. A Drug stability study using surface-enhanced Raman scattering on silver nanoparticles. Appl. Sci. 12 (4) https://doi.org/10.3390/app12041807.